Model Predictive Control for Urban Traffic Signals with Stability Guarantees*

Tong Liu † Qichao Wang ‡ Hong Wang § Zhong-Ping Jiang¶

Abstract

Traditional traffic signal control focuses more on the optimization aspects whereas the stability and robustness of the closed-loop system are less studied. This paper aims to establish the stability properties of traffic signal control systems through the analysis of a practical model predictive control (MPC) scheme, which models the traffic network with the conservation of vehicles based on a store-and-forward model and attempts to balance the traffic densities. More precisely, this scheme guarantees the exponential stability of the closed-loop system under state and input constraints when the inflow is feasible and traffic demand can be fully accessed. Practical exponential stability is achieved in case of small uncertain traffic demand by a modification of the previous scheme. Simulation results of a small-scale traffic network validate the theoretical analysis.

1 Introduction

As an important part of transportation systems, traffic signals control the flow of vehicles in the road traffic network at signalized intersections with the goal of minimizing delays. There are four main traffic signal control categories that are currently implemented in the field, i.e. fixed-time control, actuated control, responsive control, and adaptive control. Fixed-time control uses a pre-timed signal plan which does not change according to real-time traffic conditions. Note that a fixed-time control can have different timings through a day and in different days to meet the variation of traffic demand. Considering the randomness of the vehicle arrivals within a traffic control cycle given a certain traffic demand, actuated control employs loop detectors or virtual detection zones to detect incoming vehicles and trigger the extension or switching of signal phases. The dynamic adjustment relies on the structure of the phases. The ring-and-barrier structure is defined by National Electrical Manufacturers Association (NEMA) and employed in North America [18]. Traffic responsive control is an embedded feature in many traffic controllers. It uses real-time volume and occupancy information from advanced detectors to identify the current traffic pattern and implement an associated timing from a timing bank. Adaptive signal control achieves additional flexibility as the cycle length, offsets, and splits can be changed in real-time based on prevailing traffic conditions.

The optimization of signal splits has attracted rising attention in recent years. Based on the store-and-forward model [6], a network-wide traffic dynamic model called TUC model was developed based on the conservation law of vehicles, and a linear quadratic regulator was used to obtain the optimal splits with extra steps of finding the nearest feasible solution [5], with extensions of adaptively identifying the traffic flow dynamics [14, 20]. This two-step procedure was integrated into one step by considering a constrained optimal control problem [12]. Another way of processing constraints is to truncate the prediction horizon and solve a rolling horizon optimization problem [1]. The TUC model and the related optimal control assume that the vehicles in a road link can be served by any phase associated with that road link. However, at most arterial intersections, the vehicles waiting to turn left cannot leave the intersection with the through movement phase. A Virtual Phase-Link (VPL) concept was proposed to solve this issue as vehicles with different VPLs can be served by the associated NEMA phases [18]. The optimal control was achieved via MPC and the results, i.e., the signal splits, can be directly implemented in NEMA phase controllers safely.

Max pressure control as an adaptation of the Back-Pressure scheme in data networks was proposed to determine the duration of each phase in an acyclic way, and stability in the sense of bounded mean queue lengths, similar to the Lagrange stability [10] in control systems, is guaranteed assuming infinite storage capacity [17]. An extension with cyclic phases was presented with similar stability guarantees [11]. However, the storage is finite in practice and max pressure control

*This work has been supported in part by the U.S. Department of Energy under Contract DE-AC05-00OR22725 and in part by the National Science Foundation under Grant ECCS-2210320.

†Department of Electrical and Computer Engineering, New York University, Brooklyn, NY 11201. Email: tl3049@nyu.edu

‡National Renewable Energy Laboratory, 15013 Denver West Parkway, Golden, CO 804011. Email: Qichao.Wang@nrel.gov

§Oak Ridge National Laboratory, Oak Ridge, TN 37831. Email: wangh6@ornl.gov

¶Department of Electrical and Computer Engineering, New York University, Brooklyn, NY 11201. Email: zjiang@nyu.edu

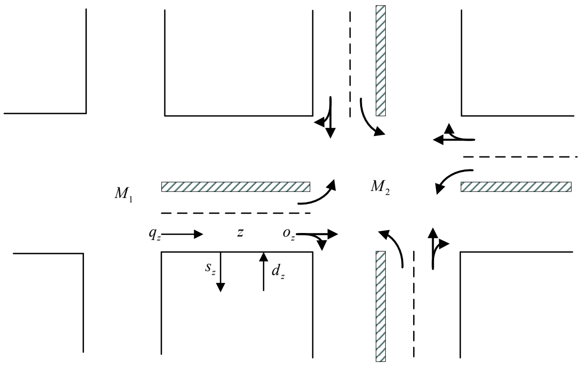

Figure 1: A virtual phase-link

can cause spillback without considering the finite storage and a capacity-aware heuristic rule was employed to improve the traffic performance [7]. There is still a lack of practical stability associated with max pressure control under finite storage capacity. Considering the finite storage constraints and phase constraints in NEMA standards, the rolling horizon optimization problem in [1] was included in an MPC scheme [18], which achieved considerable improvement over the existing actuated controller in field experiments [19]. However, the recursive feasibility of the MPC scheme [15], and the stability of the closed-loop system with the MPC scheme are still unknown. This paper fills the gaps and establishes the exponential stability in the nominal case and the practical exponential stability considering a small disturbance for the closed-loop traffic signal control system.

The rest of the paper is organized as follows. The store and forward model with constraints is presented in Section 2. The MPC scheme is introduced in Section 3. Then, recursive feasibility of the MPC scheme and stability properties of the closed-loop system are analyzed in Section 4. Simulation results are presented in Section 5. Finally, some concluding remarks are drawn in Section 6.

2 Traffic Flow Model

This section presents the traffic network model and the related state and control constraints.

The store and forward model as a macroscopic traffic flow model was proposed in [6] to describe the flow dynamics under oversaturated traffic conditions. The traffic network can be described as a directed graph where all the incoming VPLs are directed edges and traffic is transported via the connected edges in the graph (see the definition of VPLs in [18]). As shown in Fig. 1, z is an incoming VPL to intersection M_2 and vehicles can run through link z to the downstream links. There can be multiple intersections in the network. Assuming there exist n incoming VPLs in the network, the associated routing matrix $T \in \mathbb{R}^{n\times n}$ is defined as follows: for any $z, w \in \{1, ..., n\}$, $T_{[z,w]} = t_{w,z}$ where $T_{[z,w]}$ denotes the element in the z-th row and w-th column of T; $t_{w,z} \in [0, 1]$ is the turning rate from link w to link z and $t_{w,z} = 0$ if there is no direct connection between link w and link z. Besides, Let $t_{i,0} \in [0, 1]$ denote the exit rate of link i leaving the network and $T_0 = \mathrm{diag}(t_{i0}) \in \mathbb{R}^{n\times n}$ be a diagonal matrix with t_{i0} on the diagonal. A fundamental property of the network is assumed throughout the paper [4].

Assumption 2.1. *The network is outflow-connected, that is, there exists a directed path for every link to leave the network, or equivalently, to a link w with a positive exit rate $t_{w,0} > 0$.*

A consequence of Assumption 2.1 is the characterization of the eigenvalues of T.

Lemma 2.1. *[4] Under Assumption 2.1, the spectrum radius of T is less than one.*

Using this lemma, we can obtain the following result.

Proposition 2.1. *Under Assumption 2.1, let $R = (I - T_0)T$ with I denoting the identity matrix with the compatible size. Then, the spectrum radius of R is less than one.*

Proof. The corresponding graph of matrix $(I - T_0)T$ is outflow-connected, and the result follows from Lemma 2.1. □

A result of Corollary 2.1 is that

$$(I - R)^{-1} = I + R + R^2 + \cdots \geq 0 \tag{2.1}$$

which means that each element of $(I - R)^{-1}$ is non-negative since R is a non-negative matrix. Without loss of generality, the sampling time is assumed to be the cycle time C, and all intersections of the network use the same cycle time. Based on the conservation law of traffic, as shown in Fig. 1,

$$x_z(k+1) = x_z(k) + q_z(k) - s_z(k) + d_z(k) - o_z(k) \tag{2.2}$$

where $x_z(k)$ denotes the number of vehicles at link z at moment k; From time k to time $k + 1$ and for link z, $q_z(k)$ is the inflow; $s_z(k) = t_{z,0}q_z(k)$ is the local exit flow; $d_z(k)$ is the local demand flow; $o_z(k) = S_zG_z(k)$ is the outflow where $G_z(k)$ is the link green time [1] and $S_z > 0$ is the saturation rate. Let $x(k) = [x_1(k), ..., x_n(k)]^T$, $d(k) = [d_1(k), ..., d_n(k)]^T$, and $G(k) = [G_1(k), ..., G_n(k)]^T$, then

$$x(k + 1) = x(k) - (I - R)SG(k) + d(k) \tag{2.3}$$

where S is a diagonal matrix whose i-th diagonal element is S_i. Let $P \in \mathbb{R}^{n\times m}$ where m is the total number of phases for the whole network, then, for $z \in \{1, ..., n\}$ and $i \in \{1, ..., m\}$,

$$P_{[z,i]} = \begin{cases} 1, & \text{if link } z \text{ is served in phase } i, \\ 0, & \text{Otherwise.} \end{cases} \tag{2.4}$$

Compatible with P, $u(k) = [g_1(k), ..., g_m(k)]^T$ where $g_i(k) > 0$ denotes the green time for phase i with $i \in \{1, ..., m\}$. It is suggested that the order of $x_z(k)$ and $g_i(k)$ be consistent with the order of intersections so that P is a block diagonal matrix [17]. Besides,

$$0 \le G(k) \le Pu(k) \tag{2.5}$$

which is equivalent to $0 \le G_i(k) \le P_{[i,\cdot]}u(k)$ for $i \in \{1, ..., n\}$ with $P_{[i,\cdot]}$ denoting the i-th row of P. Phase time $u(k)$ is constrained by the minimum and maximum green times as

$$u_{\min} \le u(k) \le u_{\max} \tag{2.6}$$

where $u_{\min} = [g_{1,\min}, ..., g_{m,\min}]^T$ and $u_{\max} = [g_{1,\max}, ..., g_{m,\max}]^T$ with $g_{i,\min}$ and $g_{i,\max}$ denoting the minimum and maximum green times for $i \in \{1, ..., m\}$, respectively. Furthermore, NEMA standards impose additional constraints [18] as

$$Fu(k) = f \tag{2.7}$$

where $F \in \mathbb{R}^{p\times m}$ and $f \in \mathbb{R}^p$ with p denoting the total number of constraints for ring-barrier structures and cycle lengths. In addition, state constraints are considered as

$$0 \le x(k) \le x_{\max} \tag{2.8}$$

where $x_{\max} = [x_{1,\max}, ..., x_{n,\max}]^T$ with $x_{i,\max}$ denoting the storage capacity of link i for $i \in \{1, ..., n\}$. Finally, let $x^* \in \mathbb{R}^n$ denote the given set point with $0 \le x^* < x_{\max}$, and state error $\tilde{x}(k) = x(k) - x^*$. Then, (2.3) can be rewritten as

$$\tilde{x}(k+1) = \tilde{x}(k) - HG(k) + d(k) \tag{2.9}$$

with $H = (I - R)S$. Besides, an equivalent representation of (2.8) is

$$-x^* \le \tilde{x}(k) \le x_{\max} - x^*. \tag{2.10}$$

3 Model Predictive Controller

This section presents the model predictive controller considering the dynamics and constraints in Section 2.

In the remainder of this paper, for notational simplicity, denote $\tilde{x}(k)$, $x(k)$, $G(k)$, $d(k)$ and $u(k)$ as $\tilde{x}_k$, x_k, G_k, d_k, and u_k, respectively, and I_i refers to the identity matrix with size i. The following optimization problem is considered:

$$\begin{aligned} \min_{\substack{G_0,...,G_{N-1} \\ u_0,...,u_{N-1}}} \quad & \tilde{x}_N^T Q_f \tilde{x}_N + \sum_{k=0}^{N-1} \tilde{x}_k^T Q \tilde{x}_k \\ \text{s.t.} \quad & (2.5), (2.6), (2.7), (2.9),\ k = 0, ..., N-1 \\ & (2.10),\ k = 1, ..., N \end{aligned} \tag{3.11}$$

where $Q \in \mathbb{R}^{n\times n}$ is a diagonal matrix whose i-th diagonal element is $1/x_{i,\max}^2 > 0$ with $i \in \{1, ..., n\}$; $Q_f \in \mathbb{R}^{n\times n}$ is positive definite; The integer $N > 1$ refers to the planning horizon. The objective function is aimed at balancing the traffic densities over different links and the role of Q_f will be clear in the next Section. When $x^* = 0$ and $Q_f = Q$, the problem (3.11) is the same as the optimization problem in [18], and degenerates to the problem in [1] without considering (2.7).

Initial state $\tilde{x}_0$ is assumed to satisfy (2.10) and is not considered in the constraints of (3.11). The MPC requires that at each moment k, when a new state $\tilde{x}_0$ is received, the optimization problem (3.11) will be solved and any one of the optimal solutions $(G_0^*; u_0^*; ...; G_{N-1}^*; u_{N-1}^*)$ is chosen, from which $(G_0^*; u_0^*)$ is taken as the control input from time k to time $k+1$. In practice, usually only green time u_0^* can be applied and G_0 is automatically decided, and the difference $G_0 - G_0^*$ can be regarded as a disturbance to the nominal system, and the robustness result in Section 4 is still applicable. (3.11) turns out to be a quadratic programming problem that can be solved efficiently.

Proposition 3.1. *Problem (3.11) is a quadratic programming problem, that is, the objective function is convex and quadratic, and the constraints are linear over the decision variables.*

Proof. Let $U_k = [G_k^T, u_k^T]^T$, $\bar{U}_k = [U_0^T, ..., U_k^T]^T$, $\bar{X}_k = [\tilde{x}_1^T, ..., \tilde{x}_k^T]^T$, $\bar{d}_k = [d_0^T, ..., d_k^T]^T$, and $\tilde{H} = [H, 0] \in \mathbb{R}^{n\times(n+m)}$. Then $\bar{U}_{N-1}$ is the decision variable. From (2.9), we have

$$\bar{X}_N = \bar{X}_N^0 - (\Delta_N \otimes \tilde{H})\bar{U}_{N-1} + (\Delta_N \otimes I_n)\bar{d}_{N-1} \tag{3.12}$$

where $\Delta_N \in \mathbb{R}^{N\times N}$ is a lower triangular matrix with each lower triangular element being 1; $\otimes$ is Kronecker product; $\bar{X}_N^0 = \mathbf{1}_N \otimes \tilde{x}_0$ with $\mathbf{1}_N \in \mathbb{R}^N$, each of whose elements is 1. Through (3.12), each constraint in (3.11) is a linear equality or inequality over $\bar{U}_{N-1}$. Besides, the cost function becomes

$$J(\bar{U}_{N-1}) = \bar{U}_{N-1}^T M \bar{U}_{N-1} + a^T \bar{U}_{N-1} + b \tag{3.13}$$

where $a \in \mathbb{R}^{N(m+n)}$ and $b \in \mathbb{R}$ are constant vectors that are irrelevant to $\bar{U}_{N-1}$. In addition, $M = M_1 + M_2$ with

$$M_1 = \begin{bmatrix} (\Delta_{N-1} \otimes \tilde{H})^T (I_{N-1} \otimes Q)(\Delta_{N-1} \otimes \tilde{H}) & 0 \\ 0 & 0 \end{bmatrix}$$

and

$$M_2 = (1_N^T \otimes I_{m+n})^T \tilde{H}^T Q_f \tilde{H} (1_N^T \otimes I_{m+n}).$$

M is positive semi-definite since Q and Q_f are positive definite. Because the Hessian matrix $\nabla^2 J(\bar{U}_{N-1}) = 2M$ is positive semi-definite, $J(\bar{U}_{N-1})$ is a convex function over $\bar{U}_{N-1}$, which competes the proof. ∎

4 Stability Analysis

This section presents the stability analysis of the closed-loop system under the given MPC scheme and gives the robustness result when the nominal system is perturbed with a small disturbance.

It is known that any network can only accommodate finite demand and it is necessary to make appropriate assumptions on the time-varying demand vector d_k. Denote $\Omega = \{u \in \mathbb{R}^m | u_{\min} \le u \le u_{\max}, Fu = f\}$.

Definition 4.1. *The set of feasible flows with positive parameters $\varepsilon_1, \varepsilon_2$ of a network under flow dynamics (2.9) and constraints (2.5), (2.6), (2.7), (2.10) is*

$$D(\varepsilon_1, \varepsilon_2) = \{d \in \mathbb{R}_+^n | \varepsilon_1 H^{-1} x^* \le H^{-1} d \le Pu - \varepsilon_2 \mathbf{1}_n, \text{ for some } u \in \Omega\}$$

Remark 4.1. *The constant ε_2 describes the intensities of the inflows, e.g., with a larger ε_2, the intensity is smaller. The left-side term is proposed to keep the steady state x^* with appropriate inflows, and the inequality degenerates to the trivial case $H^{-1}d \ge 0$ when $x^* = 0$, in which ε_1 can be chosen arbitrarily large. Besides, the feasible flow is fully decided by the network structure, steady states, and signal configurations, and is not related to the internal states. In addition, this condition can be regarded as a counterpart of feasible flows for continuous-time systems in [13] when $x^* = 0$.*

A series of results arise from Definition 4.1, and one is the emergence of a stabilizing controller decided by the demand vector d_k and the state vector x_k as follows.

Lemma 4.1. *Assume the demand $d_k \in D(\varepsilon_1, \varepsilon_2)$ with some positive parameters $\varepsilon_1, \varepsilon_2$, that is, there exists $u_k \in \Omega$ such that $\varepsilon_1 H^{-1} x^* \le H^{-1} d_k \le Pu_k - \varepsilon_2 \mathbf{1}_n$ for $k = 0, 1, ...$, then there exists $\delta > 0$ such that u_k together with $G_k = H^{-1} d_k + \delta H^{-1} \tilde{x}_k$ renders the system (2.9) exponentially stable from any initial state $\tilde{x}_0$ satisfying (2.10), and constraints (2.5), (2.6), (2.7), (2.10) are respected for $k = 0, 1, ...$*

Proof. First, let us consider the satisfaction of constraints. For moment $k+1$, constraint (2.10) requires

$$-x^* \le \tilde{x}_k - HG_k + d_k \le x_{\max} - x^*$$

which can be satisfied as long as $0 < \delta \le 1$ since $-x^* \le \tilde{x}_k \le x_{\max} - x^*$. Besides, when

$$\delta \le \frac{\varepsilon_2}{|H^{-1} x_{\max}|_\infty}$$

where $|\cdot|_\infty$ denotes the maximum norm of a vector,

$$\begin{aligned} G_k &= H^{-1} d_k + \delta H^{-1} \tilde{x}_k \\ &\le H^{-1} d_k + \delta H^{-1} x_{\max} \\ &\le Pu_k - \varepsilon_2 \mathbf{1}_n + \delta |H^{-1} x_{\max}|_\infty \mathbf{1}_n \\ &\le Pu_k. \end{aligned}$$

In addition, when $0 < \delta \le \varepsilon_1$,

$$G_k \ge (1 - \delta/\varepsilon_1) H^{-1} d_k + \delta H^{-1} x_k \ge 0$$

by the non-negativity of H^{-1}, d_k, δ and x_k. Therefore, when $0 < \delta \le \min\{1, \varepsilon_1, \varepsilon_2 / |H^{-1} x_{\max}|_\infty\}$, constraints (2.5) and (2.10) are respected. Constraints (2.6) and (2.7) are satisfied by the existence of u_k. By the mathematical induction, constraint satisfaction is achieved for $k = 0, 1, ...$ Now let us consider the scalar Lyapunov function $V_f(x) = x^T Q_f x$ with a positive definite matrix Q_f and it satisfies

$$V_f(\tilde{x}_{k+1}) - V_f(\tilde{x}_k) = -\varepsilon_f V_f(\tilde{x}_k) \tag{4.14}$$

with $\varepsilon_f = 1 - (1 - \delta)^2$, from which $V_f(\tilde{x}_k) = (1 - \delta)^{2k} V_f(\tilde{x}_0)$ and

$$|\tilde{x}_k|_2^2 \le \frac{\lambda_{\max}(Q_f)}{\lambda_{\min}(Q_f)} (1 - \delta)^{2k} |\tilde{x}_0|_2^2$$

where $|\cdot|_2$ denotes the 2-norm of a vector (sometimes the subscript 2 is ignored), and $\lambda_{\max}(Q_f)$ and $\lambda_{\min}(Q_f)$ denote the maximum and minimum eigenvalues of Q_f, respectively. ∎

Therefore, $\tilde{x}_N^T Q_f \tilde{x}_N$ in (3.11) serves as a control Lyapunov function and it guarantees the existence of an exponentially stabilizing controller by Lemma 4.1. Next, the stability analysis is presented using the MPC proposed in Section 3.

Theorem 4.1. *Assume the demand $d_k \in D(\varepsilon_1, \varepsilon_2)$ with some positive parameters $\varepsilon_1, \varepsilon_2$ for $k = 0, 1, ...$, then there exists a positive definite matrix Q_f such that: (1) The feasibility of the problem (3.11) at $k = 0$ implies its feasibility for $k = 1, 2, ...$ (2) The closed-loop system with the MPC scheme is exponentially stable from any initial state $\tilde{x}_0$ satisfying (2.10).*

Proof. At moment k, assume one optimal solution of the problem (3.11) is $U_k^*, U_{k+1}^*, ..., U_{k+N-1}^*$ and the corresponding state sequence is $\tilde{x}_k, \tilde{x}_{k+1}^*, ..., \tilde{x}_{k+N}^*$ with $\tilde{x}_k$ satisfying (2.10). At moment $k+1$, let the control sequence be $U_{k+1}^*, ..., U_{k+N-1}^*, U_{k+N}^{'}$ with

$$U_{k+N}^{'} = \begin{bmatrix} H^{-1}d_{k+N} + \delta H^{-1}\tilde{x}_{k+N}^* \\ u_{k+N} \end{bmatrix}$$

where $0 < \delta \leq \min\{1, \varepsilon_1, \varepsilon_2/\left|H^{-1}x_{\max}\right|_\infty\}$ and $H^{-1}d_{k+N} \leq Pu_{k+N} - \varepsilon_2\mathbf{1}_n$ with $u_{k+N} \in \Omega$. The terminal state $\tilde{x}_{k+N+1} = (1-\delta)\tilde{x}_{k+N}^*$, thus $\tilde{x}_{k+N+1}$ satisfies (2.10). The other constraints are satisfied via the proof of Lemma 4.1. Thus recursive feasibility is achieved. Let the optimal cost function of problem (3.11) be the Lyapunov function $V(\tilde{x}_k) = \tilde{x}_k^T Q\tilde{x}_k + \sum_{i=1}^{N-1} (\tilde{x}_{k+i}^*)^T Q\tilde{x}_{k+i}^* + (\tilde{x}_{k+N}^*)^T Q_f\tilde{x}_{k+N}^*$ and

$$\begin{aligned} V(\tilde{x}_{k+1}^*) \leq &\sum_{i=1}^{N-1} (\tilde{x}_{k+i}^*)^T Q\tilde{x}_{k+i}^* + (\tilde{x}_{k+N}^*)^T Q\tilde{x}_{k+N}^* \\ &+ \tilde{x}_{k+N+1}^T Q_f \tilde{x}_{k+N+1} \end{aligned}$$

since the right-side term refers to the cost of a feasible control sequence. By (4.14),

$$\begin{aligned} V(\tilde{x}_{k+1}^*) - V(\tilde{x}_k) \leq &- \tilde{x}_k^T Q\tilde{x}_k + (\tilde{x}_{k+N}^*)^T Q\tilde{x}_{k+N}^* \\ &- \varepsilon_f(\tilde{x}_{k+N}^*)^T Q_f\tilde{x}_{k+N}^*. \end{aligned}$$

When $Q - \varepsilon_f Q_f$ is a negative semi-definite matrix (or equivalently $Q_f \succcurlyeq Q/\varepsilon_f$), $V(\tilde{x}_{k+1}) - V(\tilde{x}_k) \leq -\tilde{x}_k^T Q\tilde{x}_k \leq -\lambda_{\min}(Q)\left|\tilde{x}_k\right|_2^2$ since $\tilde{x}_{k+1} = \tilde{x}_{k+1}^*$ without regard to disturbances. Besides, $V(\tilde{x}_k) \geq \lambda_{\min}(Q)\left|\tilde{x}_k\right|^2$ and $V(\tilde{x}_k) \leq \tilde{x}_k^T Q_f\tilde{x}_k$ by the monotonicity of optimal value functions (see Proposition 2.18 in [15]). It follows that

$$V(\tilde{x}_{k+1}) - V(\tilde{x}_k) \leq -\gamma V(\tilde{x}_k) \tag{4.15}$$

with $\gamma = \lambda_{\min}(Q)/\lambda_{\max}(Q_f) \leq 1$ by Weyl's inequality [9] and

$$\left|\tilde{x}_k\right|_2^2 \leq \frac{(1-\gamma)^k}{\gamma}\left|\tilde{x}_0\right|_2^2$$

from any $\tilde{x}_0$ satisfying (2.10). ∎

REMARK 4.2. *As a feasible control has been found in Lemma 4.1, by Theorem 4.1, problem (3.11) is feasible for $k = 0, 1, \ldots$. Besides, when $\varepsilon_f = 1$, $Q_f = Q$ is sufficient to guarantee the exponential stability of the closed-loop system. When $\varepsilon_f < 1$, we need to choose larger Q_f such that $Q - \varepsilon_f Q_f$ is negative semi-definite, which puts more weights on the terminal cost.*

It is known that exponential stability of a nominal discrete-time system does not imply the boundness of the states even with a small disturbance [16]. For transportation systems, information on traffic demand cannot be obtained accurately. Therefore, it is necessary to consider the robustness of the nominal MPC in face of uncertainty, similar to the study of the robustness of Lagrange stability for continuous-time systems [8, 10]. In regard to the robustness analysis, the satisfaction of the state constraints (2.10) can be guaranteed by tightening the state constraints (2.10) and applying the control every N steps instead of one step [2].

COROLLARY 4.1. *Assume (2.9) is perturbed by $\tilde{d}_k$ as $\tilde{x}_{k+1} = \tilde{x}_k - HG_k + d_k + \tilde{d}_k$ with $\left|\tilde{d}_k\right|_\infty \leq \tilde{d}_{\max}$, and $d_k \in D(\varepsilon_1, \varepsilon_2)$ with some positive parameters $\varepsilon_1, \varepsilon_2$ for $k = 0, 1, \ldots$, and $x^* > 0$. Then there exist a positive definite matrix Q_f for (3.11), and a constant $\varepsilon_3 > 0$ with which the state constraints (2.10) are tightened by*

$$-x^* + \varepsilon_3\mathbf{1}_n \leq \tilde{x}(k) \leq x_{\max} - x^* - \varepsilon_3\mathbf{1}_n. \tag{4.16}$$

At time Ni with $i = 0, 1, \ldots$, problem (3.11) is solved with additional constraints (4.16) for $k = 1, 2, \ldots, N$ and one of the optimal solutions is applied to the system for the next N steps. Then, there exist $\varepsilon > 0$, $0 \leq c < 1$ and a class $\mathcal{K}_\infty$ function β such that for all initial conditions satisfying (2.10), when $\tilde{d}_{\max} \leq \varepsilon$, recursive feasibility is achieved with constraint satisfaction of (2.5), (2.6), (2.7) and (2.10) for $k = 0, 1, \ldots$, and

$$V(\tilde{x}_{k+N}) \leq cV(\tilde{x}_k) + \beta(\varepsilon). \tag{4.17}$$

for $k = Ni$, $i = 0, 1, \ldots$.

Proof. At moment k, let $0 < \delta \leq \min\{1, \varepsilon_1, \varepsilon_2/\left|H^{-1}x_{\max}\right|_\infty\}$, $H^{-1}d_{k+i} \leq Pu_{k+i} - \varepsilon_2\mathbf{1}_n$ with $u_{k+i} \in \Omega$, and $G_{k+i} = H^{-1}d_{k+i} + \delta H^{-1}\tilde{x}_{k+i}$, for $i = 0, \ldots, N-1$. When $\varepsilon_3 \leq \delta[x^*]_{\min}$ with $[x^*]_{\min}$ denoting the minimum component of x^*, one has $\varepsilon_3\mathbf{1}_n \leq \delta x^*$ and $-x^* + \varepsilon_3\mathbf{1}_n \leq -(1-\delta)x^*$. Similarly, when $\varepsilon_3 \leq \delta[x_{\max} - x^*]_{\min}$, one has $\varepsilon_3\mathbf{1}_n \leq \delta(x_{\max} - x^*)$ and $(1-\delta)(x_{\max} - x^*) \leq x_{\max} - x^* - \varepsilon_3\mathbf{1}_n$. Therefore, when G_{k+i}, u_{k+i} are applied with $i = 0, \ldots, N-1$ and $\tilde{x}_k$ satisfies (2.10), the nominal state sequence $\tilde{x}_{k+i}^{'}$ satisfies (4.16) for $i = 0, \ldots, N-1$, if $\varepsilon_3 \leq \min\{\delta[x^*]_{\min}, \delta[x_{\max} - x^*]_{\min}\}$. G_{k+i} and u_{k+i} satisfy constraints (2.5), (2.6) and (2.7) via the proof of Lemma 4.1. Thus one feasible control sequence has been found for the modified problem.

Assume one optimal solution of the modified problem is $U_k^*, U_{k+1}^*, \ldots, U_{k+N-1}^*$ and the corresponding nominal state sequence is $\tilde{x}_k, \tilde{x}_{k+1}^*, \ldots, \tilde{x}_{k+N}^*$, of which each state satisfies (2.10) strictly. For $i = 1, \ldots, N$, the perturbed state $\tilde{x}_{k+i} = \tilde{x}_{k+i}^* + \sum_{j=0}^{i-1} \tilde{d}_{k+j}$, and when $\tilde{d}_{\max} \leq \varepsilon$

with $\varepsilon = \varepsilon_3/N$, $\tilde{x}_{k+i}$ satisfies (2.10). Control constraints (2.5), (2.6) and (2.7) are satisfied via the feasibility of the problem. Since $\tilde{x}_{k+N}$ satisfies (2.10), there exists a feasible control sequence from time $k+N$ to time $k+2N-1$. By the mathematical induction, the recursive feasibility of the modified problem is guaranteed with constraint satisfaction of (2.5), (2.6), (2.7), and (2.10) for $k = 0, 1, ...$, when $\tilde{d}_{\max} \leq \varepsilon$.

Let $V(x)$ denote the optimal cost function for the modified problem and $Q_f \succcurlyeq Q/\varepsilon_f$ with $\varepsilon_f = 1-(1-\delta)^2$, from which $\varepsilon_f x^T Q_f x \geq x^T Q x$ for any $x \in \mathbb{R}^n$. Similar to the proof of Theorem 4.1, $x^T Q x \leq V(x) \leq x^T Q_f x$ for any x satisfying (2.10), from which $\lambda_{\min}(Q)\left|x\right|_2^2 \leq V(x) \leq \lambda_{\max}(Q_f)\left|x\right|_2^2$. Besides, for $k = Ni$, $i = 0, 1, ...$,

$$V(\tilde{x}_{k+N}) - V(\tilde{x}_k) \leq \tilde{x}_{k+N}^T Q_f \tilde{x}_{k+N} - (\tilde{x}_{k+N}^*)^T Q_f \tilde{x}_{k+N}^* - \sum_{j=0}^{N-1} (\tilde{x}_{k+j}^*)^T Q \tilde{x}_{k+j}^*.$$

Since $x^T Q_f x$ is a continuous function over x, by Proposition 3.4 in [15], there exists a class $\mathcal{K}_\infty$ function α such that $\left|\tilde{x}_{k+N}^T Q_f \tilde{x}_{k+N} - (\tilde{x}_{k+N}^*)^T Q_f \tilde{x}_{k+N}^*\right| \leq \alpha(\left|\tilde{x}_{k+N} - \tilde{x}_{k+N}^*\right|)$, from which

$$\begin{aligned} V(\tilde{x}_{k+N}) &\leq V(\tilde{x}_k) - \tilde{x}_k^T Q \tilde{x}_k + \alpha(\left|\sum_{j=0}^{N-1} \tilde{d}_{k+j}\right|) \\ &\leq cV(\tilde{x}_k) + \beta(\varepsilon) \end{aligned}$$

where $c = 1 - \lambda_{\min}(Q)/\lambda_{\max}(Q_f)$ and $\beta(\cdot) = N\alpha(\cdot)$. □

REMARK 4.3. *Constant ε_3 provides an upper bound for constraint tightening to guarantee the feasibility of the perturbed states. Besides, (4.17) implies*

$$\left|\tilde{x}_k\right|_2^2 \leq \frac{\lambda_{\max}(Q_f)}{\lambda_{\min}(Q)} c^i \left|\tilde{x}_0\right|_2^2 + \frac{1}{\lambda_{\min}(Q)} \sum_{j=0}^{i-1} c^j \beta(\varepsilon)$$

for $k = Ni$, $i = 0, 1, ...$, which guarantees practical exponential stability of the closed-loop system [3]. In addition, $\tilde{x}_k$ converges exponentially to the set

$$\{\tilde{x}_k | \left|\tilde{x}_k\right|_2^2 \leq \frac{1}{\lambda_{\min}(Q)(1-c)} \beta(\varepsilon)\}$$

whose size increases with the noise level ε. Furthermore, $\varepsilon = \varepsilon_3/N$ provides an estimate of the maximum disturbance quantitatively.

5 Applicability Studies

To validate the analysis in the previous sections, this section uses two consecutive intersections in Chattanooga, Tennessee, USA as a simulation case study, where one is the intersection of E. M. L. King Blvd and Chestnut Street, and the other is the intersection of E. M. L. King Blvd and Broad Street as shown in Fig. 2 where the numbers around the arrow tails denote the VPL indices and the smaller numbers around the arrowheads denote the phase indices.

Each intersection has 4 phases, i.e., phase 1, 2, 3, and 4. The phases with odd numbers are associated with "protected left turn" movements and the ones with even numbers are associated with "through" and "right turn" movements. The lost time for all the phases are 4 seconds. The minimum green times for all the even-number phases are 8 seconds and 4 seconds for all the odd-number phases. There are 15 VPLs in total, and saturation rates and storage capacities of the VPLs are in Table 1 and partial turning rates between different VPLs are in Table 2 and the other exit rates are either 1 or can be derived by Table 2. The cycle length for both intersections is 90 seconds. The demand is selected from one peak hour in the afternoon and is uniformly distributed for each cycle. The set point $x^* > 0$ is equal to the constant demand. The first step is to find ε_1 and ε_2 in Definition 4.1. It is clear that $\varepsilon_1 = 1$ and to find ε_2, the following optimization problem

$$\begin{aligned} &\min_u \ -\mathbf{1}_n^T P u \\ &\text{s.t. } Pu - \varepsilon_2 \mathbf{1}_n \geq H^{-1} d, u \in \ \Omega \end{aligned} \tag{5.18}$$

can be solved with a given ε_2. If there is no feasible solution, ε_2 should be decreased gradually until the problem can be solved. Following these steps, we find that $\varepsilon_2 = 2.85$ and $\delta = 0.036$. The initial state $x_0 = [20, 60, 18, 13, 5, 20, 19, 68, 30, 29, 10, 34, 15, 40, 23]^T$. And the plot of the state trajectory of $\tilde{x}_k$ with the controller in Lemma 4.1 is shown in Fig. 3 and all the state and control constraints are satisfied. It can be seen that the set point is reached using more than 100 steps, and the low convergence rate arises from the conservative estimate of δ. Therefore, the controller in Lemma 4.1 is of theoretical importance but far from practice. On the other hand, $\varepsilon_f = 0.071$ and we set $Q_f = 14.5Q$ and $N = 2$. The plot of the state trajectory under the MPC proposed in Section 3 is shown in Fig. 4. It can be observed that state $\tilde{x}_k$ converges to 0 within 10 steps, which shows superior performance compared with the previous stabilizing controller. Besides, $\varepsilon_3 = 0.108$ based on δ, x^* and $x_{\max} - x^*$, and $\tilde{d}_{\max} = 0.05$. And the flow dynamics is perturbed by unknown demand $\tilde{d}_k$ with $\left|\tilde{d}_k\right|_\infty \leq \tilde{d}_{\max}$, and $\tilde{d}_k$ is sampled from a uniform distribution. The modified MPC solves (3.11) with additional constraints (4.16) every 2 steps, and the solved optimal control

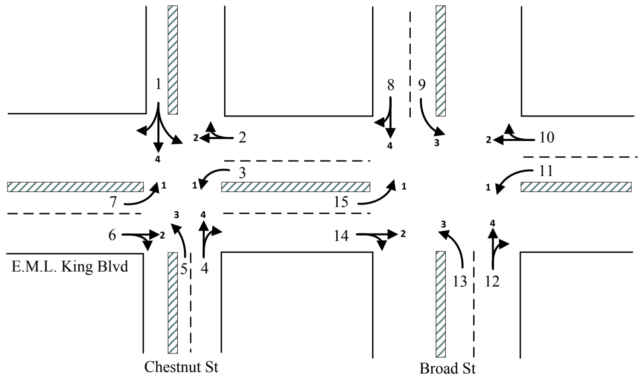

Figure 2: Layout of the intersections

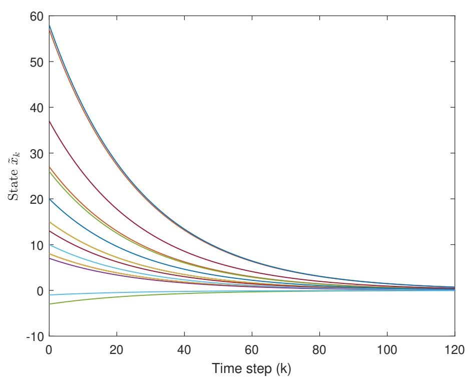

Figure 3: State trajectory using the first stabilizing controller

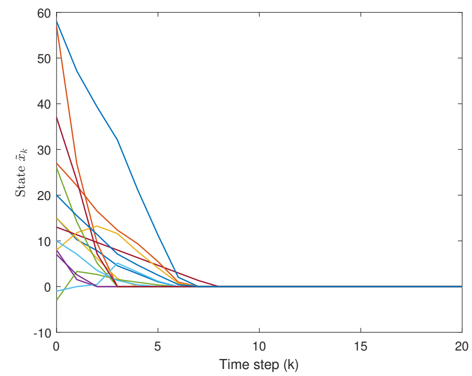

Figure 4: State trajectory using the MPC

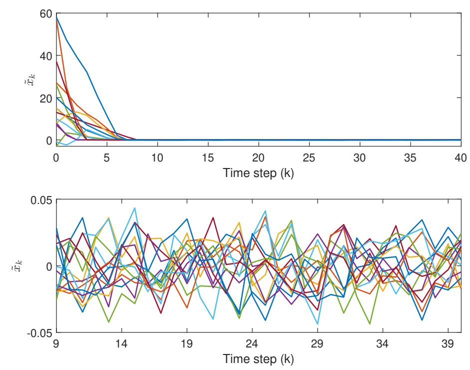

Figure 5: Perturbed state trajectory using the modified MPC

sequence is applied for the next 2 steps. The plot of the state trajectory with the unknown demand is shown in Fig. 5, and all of the constraints are satisfied during the process. It can be seen that the state $\tilde{x}_k$ is ultimately bounded with $|\tilde{x}_k|_\infty \le 0.05$. Some further experiments show that the state still keeps bounded and satisfies (2.10) when $\tilde{d}_{\max}$ and ε_3 increase together.

6 Conclusion

This paper has considered an MPC scheme for the traffic signal control problem in urban road networks. Specifically, the store and forward model is taken to describe traffic flow dynamics with the VPL concepts, and finite storage constraints and the control constraints imposed by NEMA standards are considered to formulate a quadratic programming problem in the MPC scheme aimed at balancing the traffic densities. The definition of feasible inflows is introduced and an exponentially stabilizing controller arises from this definition, with

Table 1: Properties of VPLs

VPL Id	Saturation Rate (veh/h)	Storage (veh)
1	1340	34
2	4444	70
3	1570	23
4	1580	21
5	1516	21
6	4487	66
7	1624	22
8	3369	69
9	1685	34
10	3290	41
11	1668	20
12	3209	44
13	1685	22
14	3210	47
15	1685	23

Table 2: Turning rates

Head link	Tail link	Turning rate
1	14	0.24
1	15	0.02
4	14	0.04
4	15	0.5
6	14	0.76
6	15	0.06
8	2	0.33
8	3	0.02
10	2	0.84
10	3	0.08
13	2	0.92
13	3	0.08

which the recursive feasibility and exponential stability are guaranteed for the closed-loop system with the MPC scheme. In other words, in the ideal case, the number of vehicles converges exponentially to the desired quantity for every link. In the presence of a disturbance from traffic demand, practical exponential stability guaranteeing bounded queue lengths is achieved by a modification of the MPC scheme. Finally, the simulation results based on a real-world traffic network in Chattanooga, Tennessee, USA validate the effectiveness of the theoretical analysis.

References

[1] K. Aboudolas, M. Papageorgiou, A. Kouvelas, and E. Kosmatopoulos, *A rolling-horizon quadratic-programming approach to the signal control problem in large-scale congested urban road networks*, Transportation Research Part C: Emerging Technologies, 18 (2010), pp. 680–694.

[2] J. Berberich, J. Köhler, M. A. Müller, and F. Allgöwer, *Robust constraint satisfaction in data-driven MPC*, in 2020 59th IEEE Conference on Decision and Control (CDC), IEEE, 2020, pp. 1260–1267.

[3] ——, *Stability in data-driven MPC: an inherent robustness perspective*, in 2022 IEEE 61st Conference on Decision and Control (CDC), IEEE, 2022, pp. 1105–1110.

[4] F. Bullo, *Lectures on Network Systems*, vol. 1, Kindle Direct Publishing, 2020.

[5] C. Diakaki, M. Papageorgiou, and K. Aboudolas, *A multivariable regulator approach to traffic-responsive network-wide signal control*, Control Engineering Practice, 10 (2002), pp. 183–195.

[6] D. C. Gazis and R. B. Potts, *The oversaturated intersection*, in Proceedings of the Second International Symposium on Traffic Theory, 1963, pp. 221–237.

[7] J. Gregoire, X. Qian, E. Frazzoli, A. De La Fortelle, and T. Wongpiromsarn, *Capacity-aware backpressure traffic signal control*, IEEE Transactions on Control of Network Systems, 2 (2014), pp. 164–173.

[8] W. Hahn, *Stability of Motion*, vol. 138, Springer, 1967.

[9] R. A. Horn and C. R. Johnson, *Matrix Analysis*, Cambridge University Press, 2012.

[10] Z. P. Jiang and L. Praly, *Technical results for the study of robustness of Lagrange stability*, Systems & Control Letters, 23 (1994), pp. 67–78.

[11] T. Le, P. Kovács, N. Walton, H. L. Vu, L. L. Andrew, and S. S. Hoogendoorn, *Decentralized signal control for urban road networks*, Transportation Research Part C: Emerging Technologies, 58 (2015), pp. 431–450.

[12] T. Liu, H. Wang, and Z. P. Jiang, *Data-driven optimal control of traffic signals for urban road networks*, in 2022 IEEE 61st Conference on Decision and Control (CDC), IEEE, 2022, pp. 844–849.

[13] G. Nilsson and G. Como, *Generalized proportional allocation policies for robust control of dynamical flow networks*, IEEE Transactions on Automatic Control, 67 (2020), pp. 32–47.

[14] J. Park, T. Liu, C. Wang, A. Berres, J. Severino, J. Ugirumurera, A. G. Kohls, H. Wang, J. Sanyal, and Z. P. Jiang, *Adaptive urban traffic signal control for multiple intersections: An LQR approach*, in 2022 IEEE 25th International Conference on Intelligent Transportation Systems (ITSC), IEEE, 2022, pp. 2240–2245.

[15] J. B. Rawlings, D. Q. Mayne, and M. Diehl, *Model Predictive Control: Theory, Computation, and Design*, vol. 2, Nob Hill Publishing Madison, WI, 2017.

[16] A. R. Teel, *Discrete time receding horizon optimal control: Is the stability robust?*, in Optimal Control, Stabilization and Nonsmooth Analysis, Springer, 2004, pp. 3–27.

[17] P. Varaiya, *Max pressure control of a network of signalized intersections*, Transportation Research Part C: Emerging Technologies, 36 (2013), pp. 177–195.

[18] Q. Wang and M. Abbas, *Optimal urban traffic model predictive control for NEMA standards*, Transportation Research Record, 2673 (2019), pp. 413–424.

[19] Q. Wang, J. Severino, H. Sorensen, J. Sanyal, J. Ugirumurera, C. Wang, A. Berres, W. Jones, A. Kohls, and R. P. R. VenkataDurga, *Deploying a model predictive traffic signal control algorithm-a field deployment experiment case study*, in 2022 IEEE 25th International Conference on Intelligent Transportation Systems (ITSC), IEEE, 2022, pp. 3564–3570.

[20] Z. Yin, T. Liu, C. Wang, H. Wang, and Z. P. Jiang, *Reducing urban traffic congestion using deep learning and model predictive control*, IEEE Transactions on Neural Networks and Learning Systems, (2023). doi: 10.1109/TNNLS.2023.3264709.